Cronfa - Swansea University Open Access Repository

1   **Spatiotemporal patterns of tree growth as related to carbon isotope fractionation in**

2   **European forests under changing climate**

3

4   **Running head:** Ecophysiology of forest growth in Europe

5

6   Tatiana A. Shestakova[1,2], Jordi Voltas[2], Matthias Saurer[3], Frank Berninger[4], Jan Esper[5], Laia

7   Andreu-Hayles[6], Valérie Daux[7], Gerhard Helle[8], Markus Leuenberger[9], Neil J. Loader[10],

8   Valérie Masson-Delmotte[7], Antonio Saracino[11], John S. Waterhouse[12], Gerhard H. Schleser[13],

9   Zdzisław Bednarz[14], Tatjana Boettger[15], Isabel Dorado-Liñán[16], Marc Filot[9†], David Frank[17],

10   Michael Grabner[18], Marika Haupt[15], Emmi Hilasvuori[19], Högne Jungner[19], Maarit Kalela-

11   Brundin[20], Marek Krąpiec[21], Hamid Marah[22], Sławomira Pawełczyk[23], Anna Pazdur[23],

12   Monique Pierre[7], Octavi Planells[24], Rūtilė Pukienė[25], Christina E. Reynolds-Henne[26], Katja T.

13   Rinne[27], Angelo Rita[28], Eloni Sonninen[19], Michel Stiévenard[7], Vincent R. Switsur[12‡], Elżbieta

14   Szychowska-Krąpiec[21], Malgorzata Szymaszek[23§], Luigi Todaro[28], Kerstin Treydte[3], Adomas

15   Vitas[29], Martin Weigl[30], Rupert Wimmer[31], Emilia Gutiérrez[24*]

16

17   [1] Woods Hole Research Center, Falmouth, MA, USA

18   [2] Department of Crop and Forest Sciences – AGROTECNIO Center, University of Lleida,

19   Lleida, Spain

20   [3] Swiss Federal Research Institute WSL, Birmensdorf, Switzerland

21   [4] Department of Forest Sciences, University of Helsinki, Helsinki, Finland

22   [5] Department of Geography, Johannes Gutenberg University, Mainz, Germany

23   [6] Tree-Ring Laboratory, Lamont-Doherty Earth Observatory of Columbia University,

24   Palisades, USA

25   [7] Laboratory for Climate and Environmental Sciences, CEA/CNRS/UVSQ, Gif-sur-Yvette,

26   France

27   [8] Helmholtz-Centre Potsdam, German Centre for Geosciences – GFZ, Potsdam, Germany

28   [9] Climate and Environmental Physics, University of Bern, Bern, Switzerland

29   [10] Department of Geography, Swansea University, Swansea, UK

30   [11] Department of Agricultural Sciences, University of Naples Federico II, Portici, Italy

31   [12] Department of Biomedical and Forensic Sciences, Anglia Ruskin University, Cambridge,

32   UK

33   [13] FZJ Research Center Jülich, Institute of Bio- and Geosciences IBG-3, Jülich, Germany

34   [14] Department of Forest Biodiversity, Agricultural University, Krakow, Poland

35 [15] Department of Isotope Hydrology, Helmholtz Centre for Environmental Research – UFZ,
36   Halle, Germany

37 [16] Forest Research Centre, National Institute for Agricultural Research and Experimentation
38   (INIA-CIFOR), Madrid, Spain

39 [17] Laboratory of Tree-Ring Research, University of Arizona, Tucson, USA

40 [18] Institute of Wood Technology and Renewable Resources, University of Natural Resources
41   and Life Sciences – BOKU, Vienna, Austria

42 [19] Laboratory of Chronology, University of Helsinki, Helsinki, Finland

43 [20] Forestry Museum, Lycksele, Sweden

44 [21] Faculty of Geology, Geophysics and Environmental Protection, AGH University of Science
45   and Technology, Krakow, Poland

46 [22] Water and Climate Unit, CNESTEN, Rabat, Morocco

47 [23] Department of Radioisotopes, Silesian University of Technology, Gliwice, Poland

48 [24] Department of Biological Evolution, Ecology and Environmental Sciences, University of
49   Barcelona, Barcelona, Spain

50 [25] Nature Research Centre, Institute of Geology and Geography, Vilnius, Lithuania

51 [26] Oeschger Centre for Climate Change Research, University of Bern, Bern, Switzerland

52 [27] Natural Resources Institute Finland (Luke), Vantaa, Finland

53 [28] School of Agricultural, Forest, Food and Environmental Sciences, University of Basilicata,
54   Potenza, Italy

55 [29] Environmental Research Centre, Vytautas Magnus University, Kaunas, Lithuania

56 [30] Holzforschung Austria, Vienna, Austria

57 [31] Institute for Natural Materials Technology, University of Natural Resources and Life
58   Sciences, Tulln, Austria

59 [†] Present address: CSL Behring AG, Bern, Switzerland

60 [‡] Deceased

61 [§] Present address: Janusz Kusocinski Sports School in Zabrze, Zabrze, Poland

62

63 [*]Corresponding author: Emilia Gutiérrez
64   Tel: +34 934037143
65   Email: emgutierrez@ub.edu

66

67

76 **Abstract**

77 *Aim*

78 To decipher continent-wide spatiotemporal patterns of forest growth dynamics and their

79 associations with carbon isotope fractionation processes inferred from tree rings as modulated

80 by climate warming in Europe.

81

82 *Location*

83 Europe and North Africa (30–70°N, 10°W–35°E).

84

85 *Time period*

86 1901–2003.

87

88 *Major taxa studied*

89 Temperate and Euro-Siberian trees.

90

91 *Methods*

92 We characterize changes in the relationship between tree productivity and carbon isotope

93 fractionation over the 20th century using a European network. Using indexed tree-ring widths

94 (TRW$_i$), we assess shifts in the temporal coherence of radial growth (synchrony) for five forest

95 ecosystems (Atlantic, Boreal, cold continental, Mediterranean and temperate). We also examine

96 whether TRW$_i$ shows increased coupling with leaf-level gas exchange, inferred from indexed

97 carbon isotope discrimination in tree-ring cellulose ($\Delta^{13}C_i$), through enhanced stomatal

98 regulation in response to amplified drought stress spreading northwards.

99

100 *Results*

101 We find spatial autocorrelation for TRW$_i$ and $\Delta^{13}C_i$ extending over up to 1,000 km among forest

102 stands. However, growth synchrony is not uniform across Europe, but increases along a

103 latitudinal gradient concurrent with decreasing temperature and evapotranspiration.

104 Latitudinally-structured relationships between TRW$_i$ and $\Delta^{13}C_i$ (changing from negative to

105 positive as latitude increased) point to drought impairing carbon uptake via stomatal regulation

106 of water losses as the main mechanism underlying synchronous forest growth in continental

107 Europe below 50°N. At the turn of this century, warming-induced effects on leaf physiology

108 increased synchrony in tree growth among European forests to unprecedented levels over the

109 last century.

110

Main conclusions

Increased growth synchrony from the first to the second half of the 20th century in Mediterranean, temperate and cold continental forests, together with a tighter relationship between TRW$_i$ and Δ^{13}C$_i$, indicate increasing drought effects on productivity across Europe. Such recent tendency towards exacerbated moisture-sensitive forest growth could override a positive effect of enhanced leaf intercellular CO_2 concentration, resulting in forthcoming declines in forest carbon gain continent-wide.

Keywords: carbon isotopes, climate change, dendroecology, drought stress, European forests, latitudinal gradients, *Pinus*, *Quercus*, stomatal control, tree rings

Introduction

Understanding the physiological mechanisms underlying variations in forest productivity is a key priority in global change research. Factors such as tree age, forest structure and management, nutrient availability, pollution and disturbance regimes influence the carbon budget of forested areas. During the last decades, however, climate change and increased atmospheric CO_2 ($_{atm}CO_2$) have largely altered the growth of natural forests (Nabuurs et al., 2013). To explore these dynamics, research efforts have been mainly confined to local ecosystems, with some representative woody species and their interactions examined at small spatial scales (Pivovaroff et al., 2016). This approach is hampered by site-dependent effects and limited representativeness of environmental conditions. A comprehensive understanding of tree functioning is urgently needed across broad regions in order to assess the potential and limits of forest carbon uptake globally (Chown, Gaston, & Robinson, 2004). Through the analysis of meaningful functional traits (Violle, Reich, Pacala, Enquist, & Kattge, 2014), the interpretation of spatiotemporal patterns of forest growth variability can provide comprehensive insights into the environmental responses that may change forest's services for carbon storage in the next decades (Anderegg et al., 2016).

The mechanisms and processes influencing forest productivity are extremely variable (Gibert, Gray, Westoby, Wright, & Falster, 2016). Despite such complexity, regionally coherent multispecies responses have been linked to global change effects on forest ecosystems using tree-ring networks (Babst et al., 2013; Shestakova et al., 2016). Dendroecological studies rely on the presence of common signals archived in tree populations, which are often derived from ring-width series reflecting variations in environmental factors (Fritts, 2001). Alternatively, stable isotopes are proxies of ecophysiological traits that are valuable to assess plant carbon and water relations at large spatiotemporal scales (Werner et al., 2012; Frank et al., 2015). In particular, the carbon isotope discrimination ($\Delta^{13}C$) of tree rings reflect more directly the complex array of physiological responses to environmental conditions than classical dendrochronological traits such as ring-width (Treydte et al., 2007; Gessler et al., 2014). The ratio of the heavy to light carbon isotopes ($^{13}C/^{12}C$) of organic matter depends on factors affecting CO_2 assimilation, which is mainly controlled by photosynthetic rate (A) and stomatal conductance (g_s) (Farquhar, Ehleringer, & Hubick 1989). Hence, the interannual variation in $\Delta^{13}C$ can be evaluated and retrospectively related to leaf-level physiological processes (e.g., Andreu-Hayles et al., 2011; Shestakova, Aguilera, Ferrio, Gutiérrez, & Voltas, 2014). This is especially relevant in temperate forests thriving under near-optimal conditions, where tree growth patterns may not be informative of climate variability, but stable isotopes have been

shown to be sensitive to environmental variables (Hartl-Meier et al., 2015). Indeed, much complementary information can be gained by analysing carbon isotopes in addition to ring-widths (Cernusak & English, 2015), which together provide relevant evidence on how trees respond to climate change and increasing $_{atm}CO_2$ (Andreu-Hayles et al., 2011; Saurer et al., 2014).

In drought-prone environments, tree-ring $\Delta^{13}C$ can be mainly related to the stomatal control of CO_2 fluxes into the leaf, integrating any environmental variable affecting stomatal conductance (Gessler et al., 2014). Under such conditions, radial growth and $\Delta^{13}C$ are bound together by two factors: stomatal regulation and water availability. However, $\Delta^{13}C$ is also affected by changes in photosynthetic activity associated with irradiance, phenology, nutritional stresses or N deposition when water becomes less limiting (Livingston et al., 1998). By combining ring-width and $\Delta^{13}C$, information can be gained on the array of tree performances that underlie biogeographical interactions, as these traits share spatial responses to drought events (Voelker, Meinzer, Lachenbruch, Brooks, & Guyette, 2014).

In the present study, we attempt to characterize the degree of dependence of stem growth on photosynthetic carbon isotope fractionation across European forests using a unique tree-ring network (Treydte et al., 2007). So far, only the isotope data of this network have been analysed, but not radial growth, nor the relationship between the two parameters. We used 20 chronologies from old trees comprising conifers (*Pinus*) and oaks (*Quercus*) spanning the 20th century and ranging from Mediterranean to Boreal latitudes (37°N to 69°N). Indeed, latitudinal gradients are extremely relevant for the analysis of large-scale patterns of trait variability and their relationships with ecosystem functioning (Violle et al., 2014). We hypothesise that, on a continental scale, (*i*) the temporal coherence of radial growth in forest trees is geographically structured, with more synchronous growth to be found among cold-limited, high latitude forests than among drought-prone, low-latitude forests (Shestakova et al., 2016); (*ii*) these patterns of synchrony are linked to the relative significance of carbon assimilation and stomatal control on growth determination, as reflected by relationships between ring-widths and $\Delta^{13}C$; and (*iii*) warming-induced drought stress triggers a tighter stomatal control of water losses which, in turn, enhances synchrony in low latitude forests owing to more coordinated physiological reactions to climate. On the basis of the joint analysis of radial growth and $\Delta^{13}C$, the assessment of spatiotemporal tree responses to environmental changes may improve our understanding of growth and physiology changes experienced by European forests throughout the 20th century.

Materials and methods

Tree-ring network

We used a tree-ring dataset from the pan-European network ISONET (European Union, EVK2-2001-00237), which is comprised of 20 sites and provides a comprehensive coverage of the biogeographic conditions that are found across Europe into northern Africa (Treydte et al., 2007) (Table 1). Sites consist of old-grown forests (mean age = 454 ± 196 years [SD]) from the two main genera in Europe (*Pinus* and *Quercus*) plus *Cedrus atlantica* (Morocco). The forests originate from semiarid (Mediterranean basin), humid temperate (western-central Europe), cold continental (north-central Europe) and subarctic (Fennoscandia) climates (Table 1). The sampled trees are temperate (*Quercus petraea*, *Q. robur*) and Euro-Siberian (*Pinus nigra*, *P. sylvestris*, *P. uncinata*) taxa, with sites distributed across most of their climatic ranges (Table 1). Sampled stands spread along broad latitudinal (from 32°58'N to 68°56'N) and altitudinal (from 5 m to 2,100 m a.s.l.) gradients, with high-elevation sites concentrated in southern Europe. Conifers are the dominant species in unmanaged cold Boreal or Mediterranean zones (i.e., high-latitude or high-elevation sites), whereas oaks are mainly found in humid western and central European lowlands. The distance between sites varies from about 50 km up to 4,500 km.

Increment cores were extracted from numerous trees at each site (Table S1), and tree rings were cross-dated and measured following standard dendrochronological procedures (Cook & Kairiukstis, 1990). As a proxy for above-ground woody biomass accumulation, basal area increment (BAI) for each stand was calculated as the bi-weight site mean of BAI of individual ring-width series. Temporal trends in the BAI chronologies were estimated through the slope (*b*) of the linear regression of BAI records on time. Indexed tree-ring width (TRW$_i$) and carbon isotope discrimination ($\Delta^{13}C_i$) chronologies were obtained by high-pass filtering and autocorrelation removal (see Appendix 1 in Supporting Information). Details on tree-ring network characteristics can be found in Appendix 2. The indexed ring-width and isotope chronologies were used as input for statistical analyses. The study period was 1901–2003.

Analysis of spatial variability of tree growth

Spatial structure of tree-ring traits and climatic signals across Europe

The temporal coherence of tree-ring signals (TRW$_i$, $\Delta^{13}C_i$) among sites was characterized to determine how far such coherence extends over Europe. To this end, correlation coefficients (*r*) between pairs of chronologies, calculated over the period 1901–2003, were regressed on their geographic distance using a negative exponential function for both TRW$_i$ and $\Delta^{13}C_i$. The modified correlogram technique (Koenig & Knops, 1998) was also employed to characterize

224 the spatial autocorrelations in the network. To this end, the statistical significance of the

225 pairwise correlations among chronologies was calculated within classes located 500 km apart.

226 Chronologies located farther than 2,500 km apart were combined into a single class. Hence, six

227 classes were defined ranging from <500 to >2,500 km. To evaluate the geographic extent of

228 synchrony in climate factors, the same analysis was performed for mean annual temperature

229 and precipitation.

230

231 <u>Temporal coherence of ring-width signals</u>

232 The investigation of common TRW_i variability among chronologies (growth synchrony, $â$) was

233 performed through variance-covariance (VCOV) modelling following Shestakova et al. (2014,

234 2018) (Appendix 3.1). This approach is suited to test the presence of contrasting tree-ring

235 patterns in pre-established groups of chronologies, where particular groups can be defined

236 based on existing knowledge (Shestakova et al., 2018). Here, the 20 chronologies were

237 classified into four groups according to membership to a particular climate type following the

238 Köppen climate classification (Köppen & Geiger, 1936): Boreal (*Dfc*), cold continental (*Dfb*),

239 humid temperate (C*fb*) and Mediterranean (*Csb*) (Table 1). In turn, the humid temperate climate

240 was split into Atlantic (for western Europe chronologies) and temperate (for central Europe

241 chronologies) types. These two groups originated as the result of constraining the maximum

242 distance among sites at the group level to 1,000 km (i.e., the spatial range of coherent tree-ring

243 signals as inferred from correlograms). Therefore, five different groups were defined. Each

244 group consisted of a number of neighbouring forest stands (≥3) that ensured a solution to mixed

245 model estimates.

246   A number of variance-covariance (VCOV) models accommodating between- and

247 within-group variability were tested and compared using Akaike and Bayesian information

248 criteria for model selection, which favour parsimonious models (Burnham & Anderson, 2002).

249 The VCOV models were broad evaluation (denoting common synchrony across groups),

250 narrow evaluation (corresponding to a banded main diagonal matrix denoting perfect

251 asynchrony between groups), unstructured (a completely general covariance matrix),

252 compound symmetry (a matrix having constant variance and covariance) and variants of a

253 Toeplitz structure (a matrix allowing for different (co)variances depending on the relative

254 proximity or neighbourhood among groups). These models are described in detail in Table S2.

255 Afterwards, estimates of growth synchrony ($â$) were derived using the best VCOV model for

256 the entire period (1901–2003) (Shestakova et al., 2018). The evolution of changes in $â$ was also

257 studied for successive 50-year segments lagged one year by fitting the same VCOV models.

258   The best fitting model was independently selected for each segment. This was done to

259   characterise shifts in common TRW_i variability over time potentially related to instability in

260   the relationship between tree growth and climate factors at the high-frequency domain.

261   Significant trends were determined by using the non-parametric Kendall τ rank correlation

262   coefficient.

263

264   <u>Relationships between radial growth and carbon isotope discrimination</u>

265   The temporal (yearly) association between TRW_i and $\Delta^{13}C_i$ (hereafter, r_Y) was investigated at

266   the group level through a bivariate mixed-effects model (Appendix 3.2) (Shestakova et al.,

267   2017). Broadly speaking, this approach estimates the extent by which TRW_i and $\Delta^{13}C_i$,

268   measured on the same set of chronologies, contain overlapping information as a result of plant

269   processes related to carbon uptake and water use. Hence, the relevance of a physiological

270   attribute ($\Delta^{13}C_i$) as determinant of regional forest growth is quantified by estimating how much

271   of TRW_i variability across chronologies is associated with the variability of isotopic records.

272   We argue that this quantification is relevant for studying the variable role of a putative

273   physiological tracer of productivity across large areas. The bivariate analysis was performed

274   for the entire period (1901–2003). We also evaluated the changes in r_Y between TRW_i and $\Delta^{13}C_i$

275   chronologies for successive 50-year segments lagged one year.

276

277   *Meteorological data*

278   Monthly mean temperature, precipitation and potential evapotranspiration were used for

279   climate characterization. Meteorological variables were obtained from the nearest grid point to

280   each site of the high-resolution climate dataset (Climatic Research Unit, CRU TS 3.21; Harris,

281   Jones, Osborn, & Lister, 2014). CRU provides climate series on a $0.5° \times 0.5°$ grid-box basis,

282   interpolated from meteorological stations across the globe, and extends back to 1901. However,

283   it should be noted that climate data mainly originate from low-elevation stations. This leads to

284   remarkable differences in elevation between stations and sampling sites in mountainous

285   Mediterranean areas. To account for this discrepancy, we applied lapse rate adjustments to the

286   CRU dataset for the Mediterranean sites (<45°N) following Gandullo (1994). Potential

287   evapotranspiration was estimated from CRU records using the Hargreaves method (Hargreaves

288   & Samani, 1982).

289   Bootstrapped correlations between TRW_i or $\Delta^{13}C_i$ chronologies and monthly

290   temperature, precipitation and the Standardized Precipitation-Evapotranspiration Index (SPEI3,

291   a 3-month integrated drought index; Vicente-Serrano, Beguería, & López-Moreno, 2010) were

computed over the period 1901–2003 to examine site-specific responses to climate. To assess the temporal stability of these responses, the same analysis was conducted for the split 1901–1950 and 1951–2003 periods. To ensure that results were driven by local climate rather than by long-term trends (e.g., global warming), the climatic series exhibiting a linear trend over time were detrended by fitting a straight line and keeping the residuals of these linear fits or, otherwise, simply differencing from the mean. Climate relationships were analysed from the previous October to the current September of tree-ring formation.

Analysis of biogeographical patterns of tree performance

To characterize the spatial patterns of tree growth and its dependence on $\Delta^{13}C$, changes in growth synchrony ($\hat{a}$) and in the relationship between TRW_i and $\Delta^{13}C_i$ (r_Y) were evaluated as a function of biophysical variables through simple correlations. We used geographic (latitude, longitude and elevation) and climatic records (mean annual temperature [MAT], mean annual precipitation [MAP] and potential evapotranspiration [PET]; period 1901–2003) averaged across sites for every group. It should be noted that climatic records in the network strongly depended on geographic location: MAT decreased linearly with increasing latitude ($r = -0.61$, $P < 0.01$) and longitude (or distance inland from the Atlantic Sea) ($r = -0.50$, $P < 0.05$), but it was not related to elevation. Similarly, PET was negatively related to latitude ($r = -0.84$, $P < 0.001$) and longitude ($r = -0.58$, $P < 0.01$), and positively to elevation ($r = 0.45$, $P < 0.05$). MAP was also positively related to elevation ($r = 0.45$, $P < 0.05$). The stability of these relationships was assessed through correlation analysis for the split 1901–1950 and 1951–2003 periods.

Results

Site-level growth trends and responses to climate

Eleven sites showed positive BAI trends and one site showed a negative BAI trend (slope *b*, $P < 0.05$) for the period 1901–2003, while no significant trend was detected for seven sites (Table 1). Growth acceleration was observed at all oak sites and at three pine sites from mid and high latitudes, whereas growth significantly declined in a Mediterranean site. High summer temperatures enhanced growth in Fennoscandia, whereas summer drought often constrained growth at central and southern latitudes (as indicated by negative correlations with summer temperature and positive correlations with summer precipitation and SPEI3) (Fig. S1a–c). In addition, the positive growth responses to high winter temperatures observed at some mid- and low-latitude sites suggested co-limitation by cold winters and dry summers. In comparison,

326   more clear-cut climate signals were shared by $\Delta^{13}C_i$ records, which were especially associated

327   with summer temperatures (negatively) and summer precipitation and SPEI3 (positively)

328   (Fig. S1d–f).

329

330   *Spatial consistency of tree-ring signals*

331   Naturally, the correlations between pairs of chronologies for TRW_i decreased with increasing

332   distance between sites. This effect accounted for 29% variability of inter-site correlation

333   coefficients if subject to exponential decay (Fig. 1a). The highest correlations were found

334   between *Quercus* stands from central Europe and between *Pinus* stands from north-eastern

335   Europe ($r \geq 0.30$). Significant spatial autocorrelation was recorded up to 1,000 km, with a mean

336   correlation of 0.22 and 0.12 for sites within distances of 0–500 and 501–1,000 km, respectively

337   (Fig. 1c). A Principal Component Analysis performed on TRW_i returned five principal

338   components (PCs) that accounted for 50% of the total variance. The first PC, which explained

339   12.9% of variance, had positive loadings for all chronologies, except for one Iberian site with

340   *P. sylvestris* and the Moroccan site with *C. atlantica* (Fig. S2). The highest PC1 loadings

341   corresponded to western and central European chronologies, indicating larger growth

342   similarities compared to peripheral chronologies, located farther away from each other. The

343   second PC, which explained 11.0% of variance, was also related to the geographic location of

344   chronologies: positive PC2 loadings corresponded to south-western chronologies, while north-

345   eastern chronologies had negative loadings (Fig. S2). The remaining three PCs accounted for

346   <10% of variance and showed mixed spatial signals, indicating species-specific differences and

347   the influence of local conditions on tree growth.

348   For $\Delta^{13}C_i$ chronologies, we found an exponential decrease in coherence with distance

349   between chronology pairs accounting for 28% variability of inter-site correlation coefficients

350   (Fig. 1b). Significant spatial autocorrelations were recorded up to 1,000 km (Fig. 1d). Similarly,

351   the analysis of spatial autocorrelation in climate parameters revealed that the common signal

352   declined with distance (Fig. S3a,b) and extended >2,500 km for MAT (linear function) and up

353   to 1,000 km for MAP (decay function) (Fig. S3c,d). There was also a significant negative

354   association between the most distant sites (>2,500 km) for MAP.

355

356   *Tree growth synchrony across Europe*

357   The five climate groups identified across the network consisted of three to five chronologies

358   sharing temporal growth patterns (Fig. 2). A heterogeneous Toeplitz with two bands was the

359   best model for the period 1901–2003, indicating covariation between neighbouring groups only

360   (Table S3). Growth synchrony ($\hat{a}$) varied considerably among groups, ranging from 0.06 ± 0.01

361   (Mediterranean) to 0.36 ± 0.06 (Boreal) (mean $\pm$ SE) (Fig. 3a). The $\hat{a}$ values were unrelated to

362   the average distance between sites at the group level, with groups showing the lowest and

363   highest $\hat{a}$ having inter-site distances of 785 ± 118 km and 913 ± 119 km (mean $\pm$ SE),

364   respectively. In addition, the variable number of chronologies at the group level did not

365   influence $\hat{a}$. At the between-group level, the highest $\hat{a}$ was found between Boreal and cold

366   continental forests (0.11 ± 0.02), with progressively decreasing common signals between

367   neighbours observed southwards (Fig. 3b).

368   Differences in synchrony among groups were geographically structured and related to

369   latitude ($r = 0.96$, $P < 0.01$) and longitude ($r = 0.89$, $P < 0.05$), but not to elevation (Fig. S4). At

370   the site level, however, there were strong associations between latitude and longitude ($r = 0.65$,

371   $P < 0.01$), latitude and elevation ($r = -0.59$, $P < 0.01$), and longitude and elevation ($r = -0.44$,

372   $P < 0.10$). To check for geographic consistency in these synchrony gradients across Europe, we

373   examined an independent, larger dataset of ring-width chronologies obtained from the

374   International Tree-Ring Data Bank (Grissino-Mayer & Fritts, 1997) having the same species

375   representation ($n = 80$; 52 *Pinus* chronologies and 28 *Quercus* chronologies) (Appendix 4). In

376   this case, we also detected a strong latitudinal gradient in $\hat{a}$ (Fig. S5). Consequently, we

377   assumed that this trend was essentially independent of the particular tree-ring network under

378   consideration. The observed geographic gradient in growth synchrony was also analysed in

379   relation to the potential climatic drivers of forest performance across Europe. Notably, climate

380   variables explained most geographic variation in $\hat{a}$ among groups (Fig. S6). We found strong

381   negative relationships between $\hat{a}$ and PET, followed by MAP and MAT, which are consistent

382   with a gradual decrease in evapotranspirative demand and temperature with increasing latitude.

383

384   *Temporal changes in growth synchrony*

385   The synchrony patterns changed markedly across Europe over the 20th century. $\hat{a}$ increased at

386   low and mid latitudes (i.e., in Atlantic, Mediterranean and temperate forests), whereas it

387   decreased at high latitudes (especially in Boreal, but also in cold continental forests) (Fig. 4a).

388   Such divergent geographic trends weakened the relation between $\hat{a}$ and biogeographic factors,

389   resulting in less geographically- and climatically-dependent $\hat{a}$ values across the continent after

390   1950 (Fig. S4, S6). At the between-group level, different trends were observed depending on

391   the particular group combination. For neighbouring groups, we found a substantial decrease in

392   synchrony between Boreal and cold continental forests, whereas synchrony remained steady or

393   increased for other group combinations (Fig. 4b). A modest, albeit sizeable common signal

394 emerged among the more geographically distant group pairs after 1960 ($\hat{a} \approx$ 0.05-0.10) (Fig. 4c).

395 In fact, synchrony among forest types strongly converged across Europe in the second half of

396 the century. In contrast, we did not find changes in synchrony patterns of climate parameters

397 (MAT, MAP) throughout the 20th century (results not shown). This led us to discard the

398 possibility that the observed changes in growth synchrony had been driven by concomitant

399 fluctuations in synchrony of climate factors.

400

401 *Tree growth patterns as related to isotopic signals*

402 The temporal variability shared by TRW_i and $\Delta^{13}C_i$ (r_Y) was investigated at the group level. We

403 found very different, geographically-structured relationships between these traits. The

404 association was mainly positive (for Atlantic, cold-continental and temperate forests) or very

405 positive (for Mediterranean forests), being significantly negative for Boreal forests (Fig. 5),

406 hence following a latitudinal gradient ($r = -0.96$, $P < 0.05$) (Fig. S7). Conversely, r_Y was non-

407 significant for neither longitude nor elevation (Fig. S7). In addition, r_Y was correlated to climate

408 variables at the group level, with the strongest positive association found for both PET and

409 MAP (Fig. S8).

410 The association between TRW_i and $\Delta^{13}C_i$ changed markedly across Europe throughout

411 the 20th century. r_Y turned from negative to non-significant in Boreal forests, and changed from

412 non-significant to positive in cold-continental (recently), temperate and Mediterranean forests

413 (Fig. 6). As a result, TRW_i and $\Delta^{13}C_i$ mainly became positively related across Europe. The

414 latitudinal pattern of r_Y was also stronger in the second than in the first half of the century

415 (Fig. S7). This relationship became more dependent on PET after 1950 (Fig. S8).

416

417 **Discussion**

418 This study yields evidence for geographically-structured patterns of forest growth and its

419 associations with carbon isotope fractionation processes across Europe. Common tree growth

420 and physiology were shared by stands spread up to 1,000 km. This outcome provides a general

421 indication on the geographical extent by which climate factors influence tree performance

422 continent-wide; indeed, no other environmental driver is likely to act on the same spatial scale

423 at the high-frequency domain (Fritts, 2001).

424

425 *Geographic structure and climatic controls of tree-ring signals in European forests*

426 Differential growth responses to climate were evident across the network, with temperature-

427 sensitive growth at northern latitudes, precipitation-sensitive growth at central-southern

latitudes, and mixed signals in temperate and high-elevation European forests (Babst et al., 2013). Conversely, the extent of common climate signals present in carbon isotopes suggests a tight stomatal control of water losses and, indirectly, photosynthetic activity during summer across most of Europe (Cullen, Adams, Anderson, & Grierson, 2008). These results suggest a partial de-coupling between leaf- and stem-level processes (Jucker et al., 2017). They are consistent with current evidence supporting that carbon allocation patterns change with increasing temperature and this change varies between tree species from different biomes and functional groups (Way & Oren, 2010). Details on the nature and magnitude of carbon isotope signals across the network have been reported by Treydte et al. (2007).

Interpreting ring-width patterns continent-wide

Our results show a marked geographical organization of 20th-century growth patterns across Europe. The most conspicuous changes in synchronous tree growth occurred along a north–south gradient, with $\hat{a}$ increasing northwards concurrent with a thermal gradient of decreasing temperature and reduced evapotranspiration (Babst et al., 2013). This agrees with our hypothesis of more synchronous growth in cold-limited, high-latitude forests owing to the greater spatial homogeneity of temperature effects on tree growth in northern Europe (Düthorn, Schneider, Günther, Gläser, & Esper, 2016). It contrasts with the more geographically complex drought events occurring in central and southern Europe (Orlowsky & Seneviratne, 2014), hence resulting in substantially less synchronous growth patterns (Shestakova et al., 2016).

Notably, $\hat{a}$ increased after 1950 except in Fennoscandia, which weakened the northward trend of enhanced synchrony observed during the preceding period. This outcome suggests warming-induced climatic forcing spreading across central and southern Europe, irrespective of species and local site conditions, thus enhancing synchrony through common tree sensitivity to such emergent exogenous factor (Fig. S9). It is in line with previous findings on recent high-frequency adjustments of ring-width patterns in response to amplified drought effects on growth in temperate and semiarid regions (Latte, Lebourgeois, & Claessens, 2015; Shestakova et al., 2016). In contrast, climate warming would progressively mitigate low-temperature constraints on tree performance occurring in Boreal forests (Düthorn et al., 2016). This leads to an increasing importance of local (stand-level) effects on tree growth over time, hence triggering regional asynchrony (but see Shestakova et al., 2016). We interpret these phenomena as a sign of increasing drought effects on forest growth dynamics expanding northwards across Europe, which are concurrent with temperature trends across the study area (+0.15 to +0.35°C decade^{-1} between 1960 and 2015) (EEA, 2016).

Carbon isotope fractionation relates to spatial patterns of forest growth in Europe

We investigated the physiological mechanisms underlying geographically-structured temporal growth variability through bivariate random-effects modelling of the common temporal signal present in TRW_i and $\Delta^{13}C_i$. This approach is appropriate for investigating exogenous constraints on forest growth and physiology acting over large (continental) climate gradients, because site-level impacts on tree-ring traits (e.g., differential management, competition, soil depth and fertility, etc.) are set aside explicitly from the analysis.

The positive relationships between TRW_i and $\Delta^{13}C_i$ at low and mid latitudes suggest that stomatal limitation of leaf carbon assimilation is a key mechanism controlling tree growth synchrony south of 50°N in Europe (Fig. 5). Therefore, leaf-level physiology and tree growth are driven, to a relevant extent, by water stress at about half of the study area (including e.g., France, Austria and south of Germany and Poland) during the 20th century. Conversely, the negative relationship between TRW_i and $\Delta^{13}C_i$ in Fennoscandia indicates that photosynthesis was constrained by low temperatures/sunshine hours (Gagen et al., 2011). At cool, moist sites the main control over water-use efficiency is assimilation rate, which can be limited by either enzyme activity (photon flux) or enzyme production (leaf temperature or nitrogen availability). These limitations would increase $\Delta^{13}C$ at the expense of decreased carbon uptake, hence reducing radial growth. Although our results must be weighed against the limited spatial representativeness of the sampling network, they allow delineating broad geographical trends that so far have been difficult to ascertain continent-wide, partly due to the unsystematic and sparse nature of data collection (Saurer et al., 2014). Besides, the observed trends agree with previous studies performed across smaller areas showing strong positive ring-width *vs.* $\Delta^{13}C$ correlations for trees growing under water-limited conditions, but weak correlations at wetter and colder sites (Voelker et al., 2014; del Castillo, Voltas, & Ferrio, 2015).

Strengthening of $\Delta^{13}C$–growth relationships in response to climate change

The geographical structure of tree growth relationships with carbon isotope fractionation processes varied during the 20th century. Alongside the increase in growth synchrony observed at the temperate, cold-continental and Mediterranean groups, a change from non-significant to positive correlations suggests intensified drought impacts on tree physiology since 1950 (Saurer et al., 2014). Such warming-induced drought effects influencing stomatal regulation have been shown insufficient to decrease 20th-century transpiration, as alternative factors (e.g., lengthened growing seasons or increased leaf area) counterbalance the impacts of leaf-level gas exchange

496 processes on whole-tree physiology (Frank et al., 2015). Indeed, we found evidence of growth
497 enhancement across Europe, but mainly in oaks originating from moist temperate climates in
498 low-elevation stands. For conifers, growth stimulation was observed in some of the cold-limited
499 sites, while growth decline was found in drought-constrained Mediterranean mountains. In
500 high-latitude and high-elevation sites, the increasing growth trend could be produced by a raise
501 in photosynthetic rates, which is likely driven by a combination of rising CO_2, temperature and
502 surface radiation. However, drought stress seems to override a positive effect of enhanced leaf
503 intercellular CO_2 concentration in the Mediterranean region, resulting in no change or decline
504 in productivity (Andreu-Hayles et al., 2011).

505   In Fennoscandia, the negative ring-width dependence on $\Delta^{13}C$ vanished after 1950,
506 which suggests that an earlier photosynthetic limitation of growth driven by low temperatures,
507 high cloudiness or both factors has attenuated in recent decades. In the western Mediterranean,
508 this dependence changed abruptly from zero to nearly one after 1970. Previously, growth
509 synchrony among the group chronologies was absent, rendering a null signal shared by ring-
510 width and $\Delta^{13}C$. After 1950, a common growth signal was low but relevant: this signal was
511 essentially related to $\Delta^{13}C$ fluctuations, resulting in a highly positive correlation. Although this
512 correlation implies a tight stomatal control of common radial growth in high-mountain
513 Mediterranean forests, the limited number of chronologies and the sudden change in tree
514 performance between periods might question this interpretation. A recent study carried out in
515 Iberian mountain forests allows the downscaling of our results to a local area (Shestakova et
516 al., 2017). These authors reported that multispecies tree growth at about 1,500 m is more
517 dependent on a tighter stomatal control of water losses (inferred from $\Delta^{13}C$) since the 1980s,
518 hence resembling lower elevation stands. These results reinforce our view, although more data
519 supporting this evidence are still needed on a regional scale. Unfortunately, studies on long-
520 term shifts in radial growth related to switches of the main environmental limitations to
521 photosynthetic carbon gain are still scarce (Voelker et al., 2014).

522   To conclude, we have reported forest shifts from temperature- to moisture-sensitive
523 growth spreading northwards continent-wide and associated to latitudinal changes in tree
524 dependence on carbon isotope fractionation processes. Leaf-level physiology and radial growth
525 of trees are ultimately linked via carbon allocation strategies. Common signals imprinted in
526 ring-width and stable isotopes have been broadly reported, either along geographical gradients
527 (i.e., phenotypic plasticity; del Castillo et al., 2015), over time (i.e., temporal covariation;
528 Voelker et al., 2014; Shestakova et al., 2017; this work) or at the intraspecific level (i.e., genetic
529 correlation; Fardusi et al., 2016). These evidences support (direct or indirect) effects of carbon

uptake processes on above-ground growth. On the other hand, carbohydrates are used for various other processes than growth (e.g., maintenance, respiration, reproduction) and carbon availability is seldom considered to limit tree growth (Palacio, Hoch, Sala, Körner, & Millard, 2014; but see Wiley & Helliker, 2012), which suggests that the relationship between productivity and stable isotopes may not be straightforward (Jucker et al., 2017). Alternative physiological mechanisms related to above-ground growth may interact with photosynthetic processes; for example, a critical turgor disrupting cell growth or the appearance of hydraulic constraints under drought (Sperry, 2000), or the weakening of meristematic growth under low temperatures (Rossi et al., 2016). These mechanisms would need to be carefully assessed against stable isotope signals.

Together with climate change, the increasing $_{atm}CO_2$ may have played a role in the observed shift in growth synchrony and the stronger relation between $\Delta^{13}C$ and TRW_i. Disentangling the relative effects of climate and CO_2 fertilization on spatially structured tree-ring information is challenging because both low- and high-frequency signals overlap impacting on tree physiology, carbon allocation and above- and below-ground growth. Additional factors interacting with climate change and $_{atm}CO_2$ such as increasing nutrient limitations (Jonard et al., 2015) or atmospheric deposition (de Vries, Dobbertin, Solberg, van Dobben, & Schaub, 2014) should also be considered. A previous study on the same tree-ring network demonstrated that CO_2 fertilization has increased water-use efficiency of European forests in the 20th century (Saurer et al., 2014). However, these increments were not spatially uniform and, notably, the strongest increase was reported in response to summer drought for temperate forests in central Europe, an area in which we observe large increases in growth synchrony. These findings definitely point to an increasing impact of water stress spreading northwards across European forests. Therefore, this research demonstrates that broad-scale climatic variation jointly influences tree ecophysiology and productivity in previously unrecognized ways, and sheds more light on the ecological implications of ecosystem functioning under the new climate conditions.

557   **References**

558   Anderegg, W. R. L., Klein, T., Barlett, M., Sack, L., Pellegrini, A.F., Choat, B., & Jansen, S.

559   (2016). Meta-analysis reveals that hydraulic traits explain cross-species patterns of

560   drought-induced tree mortality across the globe. *Proceedings of the National Academy*

561   *of Sciences of the United States of America*, **113**, 5024–5029.

562   Andreu-Hayles, L., Gutiérrez, E., Muntan, E., Helle, G., Anchukaitis, K. J., & Schleser, G. H.

563   (2011). Long tree-ring chronologies reveal 20th century increases in water-use efficiency

564   but no enhancement of tree growth at five Iberian pine forests. *Global Change Biology*,

565   **17**, 2095–2112.

566   Babst, F., Poulter, B., Trouet, V., Tan, K., Neuwirth, B., Wilson, R., Carrer, M., Grabner, M.,

567   Tegel, W., Levanič, T., Panayotov, M., Urbinati, C., Bouriaud, O., Ciais, P., & Frank,

568   D. (2013). Site- and species-specific responses of forest growth to climate across the

569   European continent. *Global Ecology and Biogeography*, **22**, 706–717.

570   Burnham, K.P., & Anderson, D.R. (2002) *Model selection and multi-model inference: A*

571   *practical information – theoretic approach*. Springer, New York 488 pp.

572   Cernusak, L. A., & English, N. B. (2015). Beyond tree-ring widths: stable isotopes sharpen the

573   focus of climate response of temperate forest trees. *Tree Physiology*, **35**, 1–3.

574   Chown, S. L., Gaston, K. J., & Robinson, D. (2004). Macrophysiology: large-scale patterns in

575   physiological traits and their ecological implications. *Functional Ecology*, **18**, 159–167.

576   Cook, E. R., & Kairiukstis, L. A. (1990). *Methods of dendrochronology: Applications in the*

577   *environmental sciences*. Dordrecht, Netherlands: Springer Netherlands.

578   Cullen, L. E., Adams, M. A., Anderson, M. J., & Grierson, P. F. (2008). Analyses of $\delta^{13}C$ and

579         $\delta^{18}O$ in tree rings of *Callitris columellaris* provide evidence of a change in stomatal

580   control of photosynthesis in response to regional changes in climate. *Tree Physiology*,

581   **28**, 1525–1533.

582   de Vries, W., Dobbertin, M. H., Solberg, H., van Dobben, H. F., & Schaub, M. (2014). Impacts

583   of acid deposition, ozone exposure and weather conditions on forest ecosystems in

584   Europe: an overview. *Plant and Soil*, **380**, 1–45.

585   del Castillo, J., Voltas, J., & Ferrio, J. P. (2015). Carbon isotope discrimination, radial growth,

586   and NDVI share spatiotemporal responses to precipitation in Aleppo pine. *Trees*, **29**,

587   223–233.

588   Düthorn, E., Schneider, L., Günther, B., Gläser, S., & Esper, J. (2016). Ecological and

589   climatological signals in tree-ring width and density chronologies along a latitudinal

590   boreal transect. *Scandinavian Journal of Forest Research*, **31**, 750–757.

591 European Environment Agency (2016). *Trends in annual temperature across Europe between*
592 *1960 and 2015*. [WWW document] URL http://www.eea.europa.eu/data-and-
593 maps/figures/decadal-average-trends-in-mean-6. [accessed 1 August 2018].

594 Fardusi, M. S., Ferrio, J. P., Comas, C., Voltas, J., Resco de Dios, V., & Serrano, L. (2016).
595 Intra-specific association between carbon isotope composition and productivity in
596 woody plants: a meta-analysis. *Plant Science*, **251**, 110–118.

597 Farquhar, G. D., Ehleringer, J. R., & Hubick, K. T. (1989). Carbon isotope discrimination and
598 photosynthesis. *Annual Review of Plant Physiology and Plant Molecular Biology*, **40**,
599 503–537.

600 Frank, D. C., Poulter, B., Saurer, M., Esper, J., Huntingford, C., Helle, G., Treydte, K.,
601 Zimmermann, N. E., Schleser, G. H., Ahlström, A., Ciais, P., Friedlingstein, P., Levis,
602 S., Lomas, M., Sitch, S., Viovy, N., Andreu-Hayles, L., Bednarz, Z., Berninger, F.,
603 Boettger, T., D'Alessandro, C. M., Daux, V., Filot, M., Grabner, M., Gutierrez, E.,
604 Haupt, M., Hilasvuori, E., Jungner, H., Kalela-Brundin, M., Krapiec, M., Leuenberger,
605 M., Loader, N. J., Marah, H., Masson-Delmotte, V., Pazdur, A., Pawelczyk, S., Pierre,
606 M., Planells, O., Pukiene, R., Reynolds-Henne, C. E., Rinne, K. T., Saracino, A.,
607 Sonninen, E., Stievenard, M., Switsur, V. R., Szczepanek, M., Szychowska-Krapiec, E.,
608 Todaro, L., Waterhouse, J. S., & Weigl, M. (2015). Water-use efficiency and
609 transpiration across European forests during the Anthropocene. *Nature Climate Change*,
610 **5**, 579–584.

611 Fritts, H. C. (2001). *Tree rings and climate*. Caldwell, NJ: Blackburn Press.

612 Gagen, M., Zorita, E., McCarroll, D., Young, G. H. F., Grudd, H., Jalkanen, R., Loader, N. J.,
613 Robertson, I., & Kirchhefer, A. (2011). Cloud response to summer temperatures in
614 Fennoscandia over the last thousand years. *Geophysical Research Letters*, **38**, L05701.

615 Gandullo, J. M. (1994). *Climatología y ciencia del suelo*. Madrid, Spain: Fundación Conde del
616 Valle de Salazar.

617 Gessler, A., Ferrio, J. P., Hommel, R., Treydte, K., Werner, R., & Monson, R. K. (2014). Stable
618 isotopes in tree rings: toward a mechanistic understanding of fractionation and mixing
619 processes from the leaves to the wood. *Tree Physiology*, **34**, 796–818.

620 Gibert, A., Gray, E. F., Westoby, M., Wright, I. J., & Falster, D. S. (2016). On the link between
621 functional traits and growth rate: meta-analysis shows effects change with plant size, as
622 predicted. *Journal of Ecology*, **104**, 1488–1503.

623   Grissino-Mayer, H. D, & Fritts, H. C. (1997). The International Tree-Ring Data Bank: an
624   enhanced global database serving the global scientific community. *Holocene*, **7**, 235–
625   228.

626   Hamed, K. H., & Rao, A. R. (1998). A modified Mann Kendall trend test for autocorrelated
627   data. *Journal of Hydrology*, **204**, 182–196.

628   Hargreaves, G. H., & Samani, Z.A. (1982). Estimating potential evapotranspiration. *Journal of*
629   *the Irrigation & Drainage Division – ASCE*, **108**, 225–230.

630   Harris, I., Jones, P. D., Osborn, T. J., & Lister, D. H. (2014). Updated high-resolution grids of
631   monthly climatic observations – the CRU TS3.10 Dataset. *International Journal of*
632   *Climatology*, **34**, 623–642.

633   Hartl-Meier, C., Zang, C., Büntgen, U., Esper, J., Rothe, A., Göttlein, A., Dirnböck, T., &
634   Treydte, K. (2015). Uniform climate sensitivity in tree-ring stable isotopes across
635   species and sites in a mid-latitude temperate forest. *Tree Physiology*, **35**, 4–15.

636   Jonard, M., Fürst, A., Verstraeten, A., Thimonier, A., Timmermann, V., Potočić, N., Waldner,
637   P., Benham, S., Hansen, K., Merilä, P., Ponette, Q., de la Cruz, A. C., Roskams, P.,
638   Nicolas, M., Croisé, L., Ingerslev, M., Matteucci, G., Decinti, B., Bascietto, M., &
639   Rautio, P. (2015). Tree mineral nutrition is deteriorating in Europe. *Global Change*
640   *Biology*, **21**, 418–430.

641   Jones, H. G. (1992). *Plants and microclimate*. Cambridge, England: Cambridge University
642   Press.

643   Jucker, T., Grossiord, C., Bonal, D., Bouriaud, O., Gessler, A., & Coomes, D. A. (2017).
644   Detecting the fingerprint of drought across Europe's forests: do carbon isotope ratios
645   and stem growth rates tell similar stories? *Forest Ecosystems*, **4**, 24.

646   Köppen, W., & Geiger, R. (1936). Handbuch der klimatologie. Berlin, Germany: Gebrüder
647   Bornträger.

648   Koenig, W. D., & Knops, J. M. H. (1998). Testing for spatial autocorrelation in ecological
649   studies. *Ecography*, **21**, 423–429.

650   Kress, A., Young, G. H. F., Saurer, M., Loader, N. J., Siegwolf, R. T. W., & McCarroll, D.
651   (2009). Stable isotope coherence in the earlywood and latewood of tree-line conifers.
652   *Chemical Geology*, **268**, 52–57.

653   Latte, N., Lebourgeois, F., & Claessens, H. (2015). Increased tree-growth synchronization of
654   beech (*Fagus sylvatica* L.) in response to climate change in northwestern Europe.
655   *Dendrochronologia*, **33**, 69–77.

656　Livingston, N.J., Whitehead, D., Kelliher, F.M., Wang, Y.P., Grace, J.C., Walcroft, A.S., Byers,
657　　　　J.N., Mcseveny, T.M. & Millard, P. (1998) Nitrogen allocation and carbon isotope
658　　　　fractionation in relation to intercepted radiation and position in a young *Pinus radiata*
659　　　　D. Don tree. *Plant, Cell & Environment*, **21**, 795–803.

660　Nabuurs, G. J., Lindner, M., Verkerk, P. J., Gunia, K., Deda, P., Michalak, R., & Grassi, G.
661　　　　(2013). First signs of carbon sink saturation in European forest biomass. *Nature Climate*
662　　　　*Change*, **3**, 792–796.

663　Orlowsky, B., & Seneviratne, S. I. (2014). On the spatial representativeness of temporal
664　　　　dynamics at European weather stations. *International Journal of Climatology*, **34**,
665　　　　3154–3160.

666　Palacio, S., Hoch, G., Sala, A., Körner, C., & Millard, P. (2014). Does carbon storage limit tree
667　　　　growth? *New Phytologist*, **201**, 1096–1100.

668　Pivovaroff, A. L., Pasquini, S. C., De Guzman, M. E., Alstad, K. P., Stemke, J. S., & Santiago,
669　　　　L. S. (2016). Multiple strategies for drought survival among woody plant species.
670　　　　*Functional Ecology*, **30**, 517–526.

671　Rossi, S., Anfodillo, T., Čufar, K., Cuny, H. E., Deslauriers, A., Fonti, P., Frank, D., Gričar, J.,
672　　　　Gruber, A., Huang, J. G., Jyske, T., Kašpar, J., King, G., Krause, C., Liang, E., Mäkinen,
673　　　　H., Morin, H., Nöjd, P., Oberhuber, W., Prislan, P., Rathgeber, C. B., Saracino, A.,
674　　　　Swidrak, I., & Treml, V. (2016). Pattern of xylem phenology in conifers of cold forest
675　　　　ecosystems at the Northern Hemisphere. *Global Change Biology*, **22**, 3804–3813.

676　Saurer, M., Spahni, R., Frank, D. C., Joos, F., Leuenberger, M., Loader, N. J., McCarroll, D.,
677　　　　Gagen, M., Poulter, B., Siegwolf, R. T. W., Andreu-Hayles, L., Boettger, T., Dorado
678　　　　Liñán, I., Fairchild, I. J., Friedrich, M., Gutiérrez, E., Haupt, M., Hilasvuori, E.,
679　　　　Heinrich, I., Helle, G., Grudd, H., Jalkanen, R., Levanič, T., Linderholm, H. W.,
680　　　　Robertson, I., Sonninen, E., Treydte, K., Waterhouse, J. S., Woodley, E. J., Wynn, P.
681　　　　M., & Young, G. H. (2014). Spatial variability and temporal trends in water-use
682　　　　efficiency of European forest. *Global Change Biology*, **20**, 332–336.

683　Shestakova, T. A., Aguilera, M., Ferrio, J. P., Gutiérrez, E., & Voltas, J. (2014). Unravelling
684　　　　spatiotemporal tree-ring signals in Mediterranean oaks: a variance–covariance
685　　　　modelling approach of carbon and oxygen isotope ratios. *Tree Physiology*, **34**, 819–838.

686　Shestakova, T. A., Gutiérrez, E., Kirdyanov, A. V., Camarero, J. J., Génova, M., Knorre, A. A.,
687　　　　Linares, J. C., Resco de Dios, V., Sánchez-Salguero, R., & Voltas, J. (2016). Forests
688　　　　synchronize their growth in contrasting Eurasian regions in response to climate

689   warming. *Proceedings of the National Academy of Sciences of the United States of*
690   *America*, **113**, 662–667.

691 Shestakova, T. A., Camarero, J. J., Ferrio, J. P., Knorre, A. A., Gutiérrez, E., & Voltas, J. (2017).
692   Increasing drought effects on five European pines modulate $\Delta^{13}C$-growth coupling
693   along a Mediterranean altitudinal gradient. *Functional Ecology*, **31**, 1359–1370.

694 Shestakova, T. A., Gutiérrez, E., & Voltas, J. (2018). A roadmap to disentangling
695   ecogeographical patterns of spatial synchrony in dendrosciences. *Trees*, **32**, 359–370.

696 Sperry, J. S. (2000). Hydraulic constraints on plant gas exchange. *Agricultural and Forest*
697   *Meteorology*, **104**, 13–23.

698 Stuiver, M., & Braziunas, T. F. (1987). Tree cellulose $^{13}C/^{12}C$ isotope ratios and climatic
699   change. *Nature*, **328**, 58–60.

700 Treydte, K., Frank, D. C., Esper, J., Andreu, L., Bednarz, Z., Berninger, F., Boettger, T.,
701   D'Alessandro, C. M., Etien, N., Filot, M., Grabner, M., Guillemin, M. T., Gutierrez, E.,
702   Haupt, M., Helle, G., Hilasvuori, E., Jungner, H., Kalela-Brundin, M., Krapiec, M.,
703   Leuenberger, M., Loader, N. J., Masson-Delmotte, V., Pazdur, A., Pawelczyk, S.,
704   Pierre, M., Planells, O., Pukiene, R., Reynolds-Henne, C. E., Rinne, K. T., Saracino, A.,
705   Saurer, M., Sonninen, E., Stievenard, M., Switsur, V. R., Szczepanek, M., Szychowska-
706   Krapiec, E., Todaro, L., Waterhouse, J. S., Weigl, M., & Schleser, G. H. (2007). Signal
707   strength and climate calibration of a European tree-ring isotope network. *Geophysical*
708   *Research Letters*, **34**, L24302.

709 Vicente-Serrano, S. M., Beguería, S., & López-Moreno, J. I. (2010). A Multiscalar drought
710   index sensitive to global warming: the Standardized Precipitation Evapotranspiration
711   Index. *Journal of Climate*, **23**, 1696–1718.

712 Violle, C., Reich, P. B., Pacala, S. W., Enquist, B. J., & Kattge, J. (2014). The emergence and
713   promise of functional biogeography. *Proceedings of the National Academy of Sciences*
714   *of the United States of America*, **111**, 13690–13696.

715 Voelker, S. L., Meinzer, F. C., Lachenbruch, B., Brooks, J. R., & Guyette, R. P. (2014). Drivers
716   of radial growth and carbon isotope discrimination of bur oak (*Quercus macrocarpa*
717   Michx.) across continental gradients in precipitation, vapour pressure deficit and
718   irradiance. *Plant, Cell and Environment*, **37**, 766–779.

719 Way, D. A., & Oren, R. (2010). Differential responses to changes in growth temperature
720   between trees from different functional groups and biomes: a review and synthesis of
721   data. *Tree Physiology*, **30**, 669–688.

722 Werner, C., Schnyder, H., Cuntz, M., Keitel, C., Zeeman, M. J., Dawson, T. E., Badeck, F. W.,

723   Brugnoli, E., Ghashghaie, J., Grams, T. E. E., Kayler, Z. E., Lakatos, M., Lee, X.,

724   Maguas, C., Ogee, J., Rascher, K. G., Siegwolf, R. T. W., Unger, S., Welker, J.,

725   Wingate, L., & Gessler, A. (2012). Progress and challenges in using stable isotopes to

726   trace plant carbon and water relations across scales. *Biogeosciences*, **9**, 3083–3111.

727 Wiley, E. & Helliker, B. (2012). A re-evaluation of carbon storage in trees lends greater support

728   for carbon limitation to growth. *New Physiologist*, **195**, 285-289.

729

Data Accessibility Statement

731 The tree-ring data used in this study are available upon request from the authors. Contact Emilia
732 Gutiérrez (emgutierrez@ub.edu) for ring-width chronologies and Gerhard Helle (ghelle@gfz-
733 potsdam.de) for carbon isotope records.

734

Biosketch

736 Tatiana A. Shestakova is a post-doctoral researcher at the Woods Hole Research Center,
737 Falmouth, MA (USA). Her research interests include dendroecology, stable isotope
738 biogeochemistry and climate change impacts on natural forest ecosystem. Particularly, she
739 works on designing efficient inference tools and algorithms based on mixed modelling
740 principles to understand the processes underlying the complexity and diversity in tree response
741 patterns to environmental forcing and how these patterns are spatially structured across
742 biogeographical gradients.

743

FIGURE CAPTIONS

746 Figure 1. Spatial patterns of indexed tree-ring traits across Europe for the period 1901–2003:

747 **(a, c)** indexed tree-ring width (TRW$_i$), **(b, d)** indexed carbon isotope discrimination ($\Delta^{13}C_i$).

748 *(Left panels)* Pairwise correlations of tree-ring chronologies as a function of geographical

749 distance. The patterns are summarized by regressing the correlation coefficients (*r* values)

750 involving pairs of chronologies (*y*-axis) on their corresponding distance (*x*-axis) by using

751 negative exponential functions (y = be^{-cx}). Different dot colors indicate pairwise correlations

752 within and between functional groups as follows: conifers (green), oaks (orange), and mixed

753 conifer–oak (blue). Asterisks after the coefficient of determination (r^2) indicate level of

754 significance (***P < 0.001). *(Right panels)* Spatial structure of tree-ring traits across European

755 forests. The spatial autocorrelation in the tree-ring network was characterized for six

756 consecutive distance classes (listed on the *x*-axis). Mean *r* values and their statistical

757 significance (*P*) within each distance class were estimated from 1,000 randomizations.

758 Significant correlation coefficients (*P* < 0.05) are indicated by an asterisk.

759

760 Figure 2. Geographical distribution of sites, definition of groups of chronologies and synchrony

761 in radial growth at group level. Each dot identifies a chronology ($n \geq 20$ trees) according to the

762 codes shown in Table 1 (oak codes are shown in italics). Each colored encircled area identifies

763 a group of chronologies belonging to a particular climate type (see Table 1) that are separated

764 in pairs up to 1,000 km (see Fig. 1d for the distance threshold where significant radial growth

765 patterns are shared among chronologies). The corresponding growth synchrony at the group

766 level ($\hat{a}$) is shown within a rectangle. At least three neighbouring sites form a group (total

767 number of groups, $n = 5$). $\hat{a}$ values are estimated using indexed ring-width chronologies for the

768 period 1901–2003 as described in Appendix 3.1 (Supporting Information).

769

770 Figure 3. Growth synchrony across Europe. Patterns of growth synchrony ($\hat{a}$) at the within-

771 group level for the entire period 1901–2003 **(a)**. Patterns of growth synchrony ($\hat{a}$) at the

772 between-group level for the entire period 1901–2003 **(b)**. All calculations are based on indexed

773 ring-width chronologies. Groups sorted latitudinally from north to south. Error bars denote

774 standard errors.

775

776 Figure 4. Temporal trends in growth synchrony at within- and between-group levels for the

777 period 1901–2003. Growth synchrony ($\hat{a}$) is estimated for 50-year periods lagged by 5 year

following Eqs. 5 and 6 as described in Appendix 3.1 (Supporting Information). All calculations are based on indexed ring-width (TRW_i) chronologies. For the sake of visual clarity, the estimates of $\hat{a}$ are represented separately for pairs of chronologies belonging to the same group (i.e., within-group level) **(a)**, and for pairs of chronologies belonging to different groups (i.e., between-group level) for neighbouring **(b)** and non-neighbouring chronologies **(c)**. Grey lines denote the SE. Note the change in scale of the Y-axis between panels.

Figure 5. Geographical patterns of the relationship between TRW_i and $\Delta^{13}C_i$ chronologies across Europe. The correlations at the group level (r_Y) are estimated for the entire period 1901–2003. Significant associations are depicted with an asterisk ($P < 0.10$). Error bars denote standard errors.

Figure 6. Temporal trends in associations between TRW_i and $\Delta^{13}C_i$ chronologies at the group level for the period 1901–2003. The correlations (r_Y) are estimated for 50-year periods lagged by 5 year following Eq. 7 as described in Appendix 3.2 (Supporting Information). All calculations are based on indexed ring-width (TRW_i) and carbon isotope ($\Delta^{13}C_i$) chronologies. Grey lines denote the SE of r_Y. Significant correlations (correlation coefficients with 90% confidence intervals not embracing zero) are depicted as filled dots.

No	Country	Site name	Code	Species	Latitude (°N)	Longitude (°E)	Elevation (m)	MAT (°C)	MAP (mm)	PET (mm)	MA
1	Finland	Kessi, Inari	INA	*Pinus sylvestris*	68.93	28.42	150	–1.2	432	413	Ap
2	Finland	Sivak., Ilomantsi	ILO	*Pinus sylvestris*	62.98	31.27	200	2.2	573	515	Ap
3	Norway	Gutuli	GUT	*Pinus sylvestris*	62.00	12.18	800	0.7	586	512	Ap
4	Finland	Bromarv	BRO	*Quercus robur*	60.00	23.08	5	4.9	568	562	Ap
5	UK	Lochwood	LOC	*Quercus robur*	55.27	–3.43	175	7.4	1517	589	
6	Lithuania	Panemunes Silas	PAN	*Pinus sylvestris*	54.88	23.97	45	6.6	634	672	A
7	Poland	Suwalki	SUW	*Pinus sylvestris*	54.10	22.93	160	6.7	619	686	A
8	UK	Woburn Abbey	WOB	*Quercus robur*	51.98	–0.59	50	9.5	709	724	A
9	Germany	Dransfeld	DRA	*Quercus petraea*	51.50	9.78	320	7.7	723	677	A
10	UK	Windsor	WIN	*Pinus sylvestris*	51.41	–0.59	10	9.5	763	738	A
11	Poland	Niepolomice, Gibiel	NIE1	*Quercus robur*	50.12	20.38	190	8.0	676	674	Ap
12	Poland	Niepolomice, Gibiel	NIE2	*Pinus sylvestris*	50.12	20.38	190	8.0	676	674	Ap
13	France	Fontainebleau	FON	*Quercus petraea*	48.38	2.67	100	11.5	608	861	M
14	France	Rennes	REN	*Quercus robur*	48.25	–1.70	100	11.1	733	786	A
15	Austria	Lainzer Tiergarte	LAI	*Quercus petraea*	48.18	16.20	300	9.6	654	792	M
16	Austria	Poellau	POE	*Pinus nigra*	47.95	16.06	500	8.3	815	762	Ap
17	Spain	Pinar de Lillo	LIL	*Pinus sylvestris*	43.07	–5.25	1600	5.1	1505	688	Ju
28	Spain	Massis de Pedraforca	PED	*Pinus uncinata*	42.23	1.70	2100	3.9	1299	692	Ju
19	Spain	Sierra de Cazorla	CAZ	*Pinus nigra*	37.80	–2.95	1816	8.9	712	1014	M
20	Morocco	Col du Zad	COL	*Cedrus atlantica*	32.97	–5.07	2200	10.4	717	1163	A
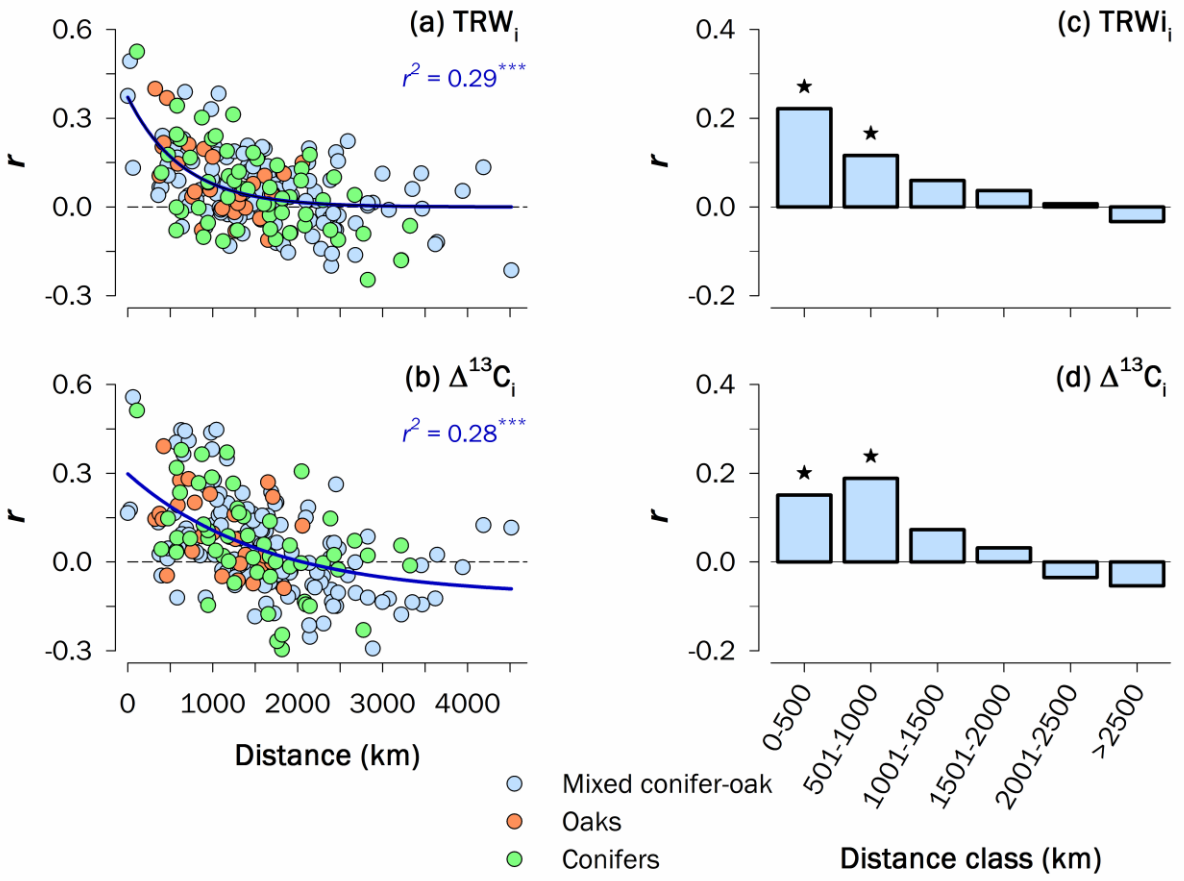
803

804 **Figure 1**

805
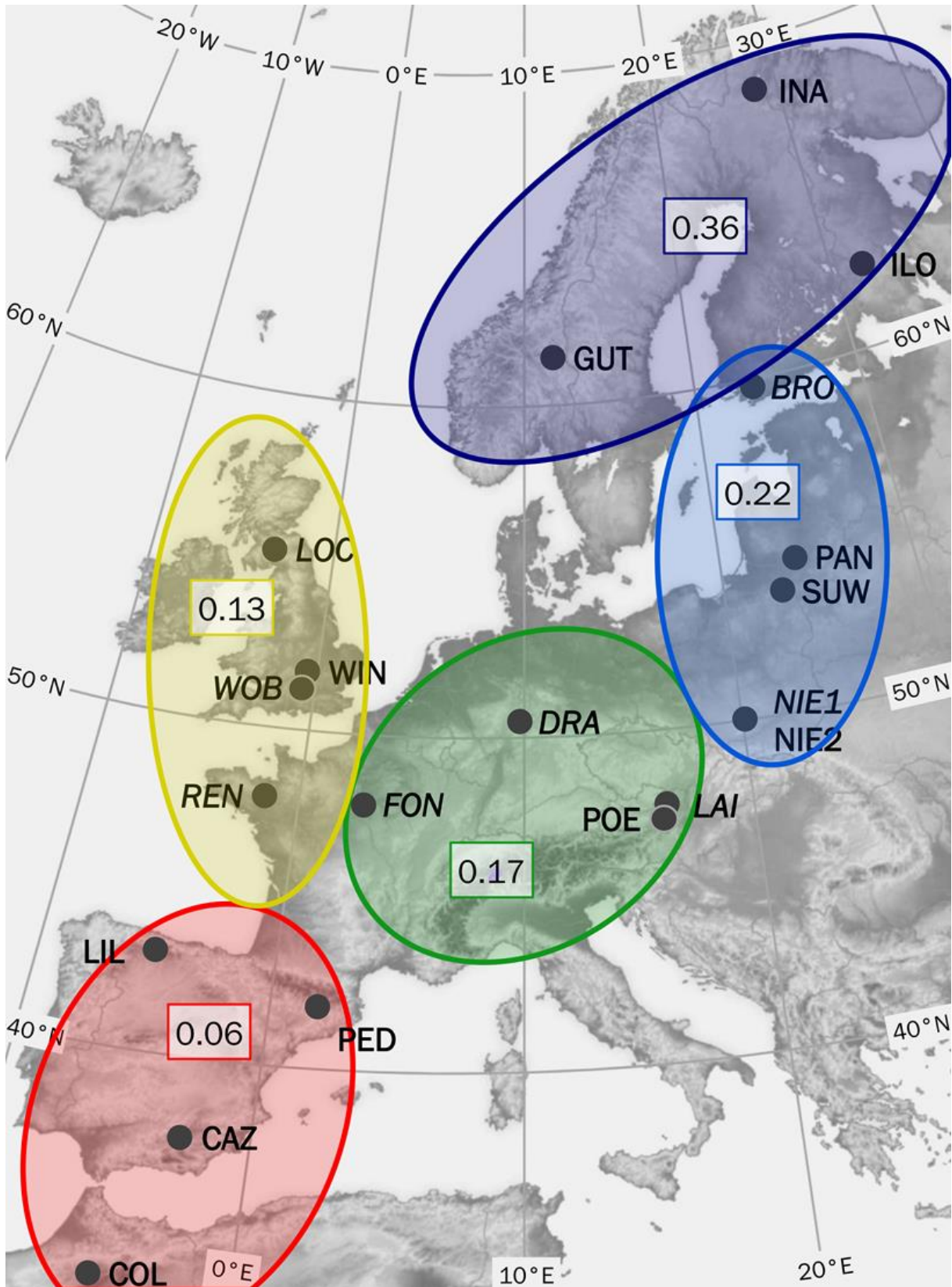
Figure 2

807

808 **Figure 3**

809

810 **Figure 4**

811

Figure 5

813

814

815 **Figure 6**